IOP Conference Series: Earth and Environmental Science

PAPER • **OPEN ACCESS**

Analysis of numerical and experimental results of a solar glazed air collector configuration in Romania climate

To cite this article: C Sima *et al* 2021 *IOP Conf. Ser.: Earth Environ. Sci.* **664** 012085

View the article online for updates and enhancements.

This content was downloaded from IP address 92.85.231.208 on 20/06/2021 at 12:17

Analysis of numerical and experimental results of a solar glazed air collector configuration in Romania climate

C Sima[1,3], **C Teodosiu**[1], **C Croitoru**[1] and **F Bode**[2]

[1] CAMBI Research Centre, Technical University of Civil Engineering Bucharest
[2] Technical University of Cluj-Napoca

simacatalin25@gmail.com

Abstract. This paper proposes an experimental and numerical study (based on CFD – Computational Fluid Dynamics technique) dealing with a glazed transpired solar collector (GTC), having the distance between the glass and absorber plate of 50 mm. The behaviour of the GTC has been studied for different air flow rates. Based on the results obtained, it can be concluded that this GTC configuration behaves best for air flow rates of about 300 m^3/h. On the other hand, further studies are needed to improve the numerical model (especially regarding the introduction of boundary conditions based on measured data).

1. Introduction

A study conducted by the IEA (International Energy Agency) shows that after the end of the covid-19 pandemic the upward trend in energy consumption is expects to growth and in 2050 is expect to be 20% to 50% more energy consumption compared to year 2020 [1,2].

The building sector is one of the largest consumers of energy and at the same time has a high contribution to greenhouse gas emissions being responsible for 36% of final energy consumption and 39% of total greenhouse gas emissions. On the other hand, according to UN Environment and the IEA - 2017 report-, energy consumption and greenhouse gases can be reduced with a minimum cost in the building sector [3].

Solar facades are promising solutions for the future of the building sector, in order to reduce energy consumption, these solutions being intensively studied internationally by achieving and optimizing different configurations of solar facades (based mainly on solar collectors). Furthermore, the integration of these solutions in buildings is increasingly studied in order to achieve better thermal performance of buildings envelopes.

Hami et al and Lai et al [4,5] classified the solar collectors according to the absorber element and obtain two main categories:

- solar collectors with flat absorber element without perforations
- solar collectors with perforated absorber element, most often in the literature this type of collector is called "transpired collector"

In addition, the solar collectors with the perforated absorber can be divided into two main categories:

- << **T**ranspired **S**olar **C**ollector (TSC) >> or simple perforated solar collector
- << **G**lazed **T**ranspired solar **C**ollector (GTC) >> or perforated solar collector with a layer of glass applied to the surface of the absorber plate

Both operating according to the same principle, the air is aspired by the fan and passes through the absorber plate, collecting the heat stored at its level. Nkwetta and Haghighat [6] present a detailed classification of all these constructive types of solar air collectors according to the solution used for thermal energy storage.

Content from this work may be used under the terms of the Creative Commons Attribution 3.0 licence. Any further distribution of this work must maintain attribution to the author(s) and the title of the work, journal citation and DOI.
Published under licence by IOP Publishing Ltd

We present in this paper experimental and numerical investigations concerning the performance of a GTC, in order to be integrated in building facades.

2. GTC experimental set-up

The main changes to the solar collector used previously at the CAMBI research center [7,11] were the use of an absorber plate with 50x50mm perforations and the use of a layer of glass over the absorber plate to reduce convection losses due to wind. Gao et al [12] mention that by reducing the diameter of the perforations from 20 mm to 10 mm the efficiency of the solar collector increased by only 0.56% and the temperature by 0.35%, so we proposed larger perforations for the solar collector arranged uniformly on the absorber plate, to simplify the manufacture of the absorber plate.

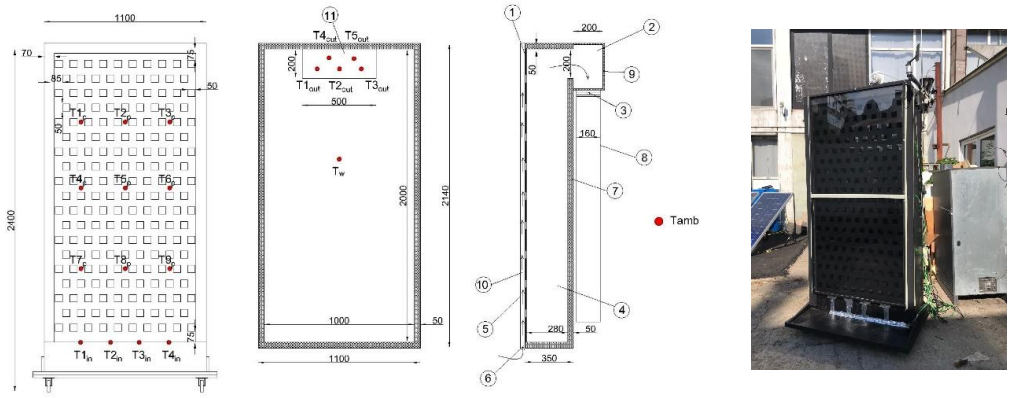

Figure 1. Design drawings and picture for experimental glazed transpired solar collector

1 – transpired plate; 2 – plenum; 3 – fan; 4 – inner cavity; 5 – glazing; 6 – air inlet; 7,9 – thermal insulation; 8 – air duct; 10 – air opening between glass and absorber; 11 – air outlet.

The solar collector was made of OSB (Oriented Strand Board) with a wooden structure - dimensions of 40x40 mm, thermally insulated with rockwool that have a thickness of 40 mm. The absorber plate was made of steel with a thickness of 2 mm and the size of 2000 mm x 1050 mm being black as well as the entire solar collector to better absorb solar radiation (thermal emissivity being considered around 0.9, value characteristic for black color). The new prototype will also include a simple 4 mm glass, that can be placed at different distances from the absorber plate (30, 50, 70 or 90 mm). In addition to this glass the solar collector was also equipped with a fan located at the exit of plenum, followed by a ventilation duct with a length of about 1.8 m.

The proposed solar collector works according to the same principle as in the case of perforated solar collectors. Thus the air is aspirated through the slot made at the bottom (point 6 in figure 1), it passes through the space created by the absorber plate and the glass layer after this the air passes through the holes made in the absorber plate, reaching the top in the suction plenum. The movement of the air is performed by a variable speed fan in order to obtain the required air flow for the solar collector.

After establishing the measurement protocol for the experimental prototype, we proceeded to the measurement stage. This was performed in the second part of October 2019 by means of Almemo 710 station. The registered parameters were the following:

- Temperature on the surface of the perforated absorber plate measured in 9 points - figure 1;
- Air temperature at the entrance to the solar collector, measured in 4 points - figure 1;
- Air temperature at the exit of the solar collector, measured in 5 points - figure 1;
- Temperature and humidity of the outside air, near the collector;

- Solar radiation, the station being placed vertical at the top of the solar collector;
- Wind speed and direction, the weather station being located at the top of the solar collector.

The measurement protocol was repeated for each day and consisted of preparing the solar collector and running its measurements from 12:00 till 18:00. The recording of experimental data was performed continuously and automatically during this period (recording step: 30 seconds). For the experimental investigation, we studied the GTC configuration with a distance of 50 mm between the absorber plate and the layer of glass for each of the following air flows: 75, 100, 125, 150, and 175 m^3 / h m^2.

The main characteristics of all experimental devices used in our study are indicated in Table 1.

Table 1. Information about the measuring devices

Device	Measured parameter	Type	Range	Accuracy
thermocouple	air / surface temperature	K (NiCr-Ni)	-10…+105ºC	±0.2ºC
air flow meter	air flow	FlowFinder mk2 system	10…550 m^3/h	3%
digital temp.sensor	ambient temperature	Almemo FHAD 46-C2	-20…+60ºC	±0.2ºC
cup anemometer	wind velocity	Almemo FVA 615 2	0.5…50 m/s	3%
wind vane	wind direction	Almemo FVA 614	0…360º	±5º
pyranometer	solar radiation intensity	Almemo FLA 628 S	0…1500 W/m^2	< 3%

3. Experimental results

We present in this section the main experimental data acquired during our study. Table 2 illustrates the average values of weather parameters during the period 1:10 p.m. - 2:10 p.m for each of 5 days of measurements (one day of measurements corresponds to an air flow rate value). This interval has been chosen as throughout this period weather parameters, especially intensity of solar radiation, have been characterised by constant values for all measurement days.

Table 2. Mean weather data for **50 mm glazing - perforated plate** tests (1:10 p.m. to 2:10 p.m.)

Parameter / Air flow rate (m^3/h,m^2)	77	102.5	127	151	175
Outdoor temperature (°C)	22.6	25.1	23.7	28.4	22.8
Solar radiation (W/m^2)	681.9	659.7	685.6	684.5	617.8
Wind speed (m/s)	0.32	0.46	0.35	0.17	0.13

The main parameters that were studied for the GTC collector were the difference between the inlet and outlet air and the temperature of the absorber plate for the 5 measurement cases. Based on data from Table 3, it can be observed that the temperature difference decreases linear with the increase of the flow.

Table 3. GTC test parameters for **50 mm glazing - perforated plate** (1:10 p.m. to 2:10 p.m.)

Parameter / Air flow rate (m^3/h,m^2)	77	102.5	127	151	175
$\Delta T_{out\text{-}in}$ (°C)	13.2	9.6	9.6	8.1	5.4
T_{plate} (°C)	52.7	48.9	44.9	43.9	39.3

In order to obtain a better comparation between the numerical and experimental results, we used the main parameters that define the thermal performance of the solar collector, heat exchange efficiency (ε HX), solar collector efficiency (η) and temperature difference between the introduced air and the exhaust air (Δ T), formulas proposed by Wang et al. [13]:

$$\eta = \frac{c_{p,air} m_{air} \left(T_{air,ev} - T_{amb}\right)}{I_T A_S} \quad (1)$$

$$\varepsilon_{HX} = \frac{T_{air} - T_{amb}}{T_P - T_{amb}} \quad (2)$$

where:

- $c_{p,air}$ - the specific heat of air (J/kg °C),
- m_{air} - the mass flow rate of air (kg/s),
- $T_{air\text{-}ev}$ - the air outlet temperature (K),
- T_{amb} - the ambient air temperature (K),
- I_T - the intensity of the solar radiation (W/m^2),
- As - the absorber area of the air solar collector (m^2),
- T_p - the absorber (plate) surface temperature (K).

The following formula was also used to calculate the heat flux:

$$Q = m_{aer} \times \rho \times c_p \times \left(T_{aer,ev} - T_{amb} \right) \quad (3)$$

For the heat flux released, the air flow rate of 300 m^3/h is the point where the heat flux released by the GTC begins to decrease and a difference of 200W can be seen in Figure 2.

The overall efficiency of the solar collector was calculated using Wang's formula (1). It was observed that the efficiency is improved for air rate flows between 250 m^3/h to 300 m^3/h (Figure 3), after 300 m^3/h the global efficiency begins to decrease.

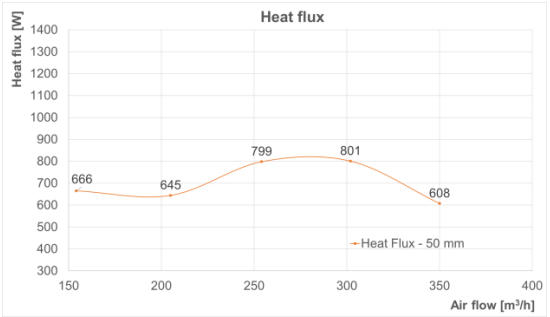

Figure 2 Heat flux released for experimental GTC

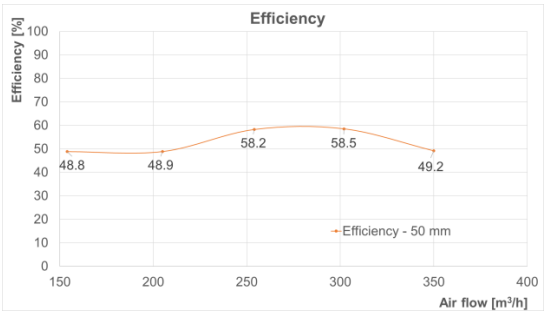

Figure 3 Global efficiency of GTC

The comparative study was completed by reporting the global efficiency to solar radiation for each air flow rate in the range 150 - 350 m^3/h (Figure 4).

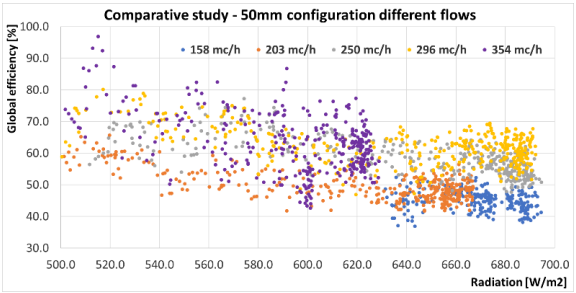

Figure 4 Global efficiency of GTC

In order to better compare the behavior of the solar collector for different air flow rates, we analyzed its global efficiency for the same values of solar intensity. It was observed that for the five cases illustrated in Figure 4, the best efficiency is reached for the 300 m^3/h air flow rate.

4. Discussion on experimental data

By implementing the glass layer on the surface of the collector, it reduces the negative impact on the efficiency of the solar collector. Thus the solar collector can be implemented as a solution for heating and ventilation of buildings in areas where we have a low temperature climate and relatively important winds.

The exponential increase of the global efficiency for the solar collector is stopped around 300 m^3/h, being a limit value that can be considered for the following experimental studies.

5. Numerical study

The numerical study for the solar collector was performed using the Ansys 19.2 commecial software. For the numerical study, the geometry was made according to the experimental study (Figure 1), the geometry was initially made in the SolidWorks program and then imported into the Ansys program.

After generating different meshes, the following configurations were chosen as mesh studies: 0.714, 1.45, 2.95 and 4.13 million tetrahedral elements. Based on the mesh independence study, it was observed that the mesh with 2.95 million elements has led to the best results (Figure 5).

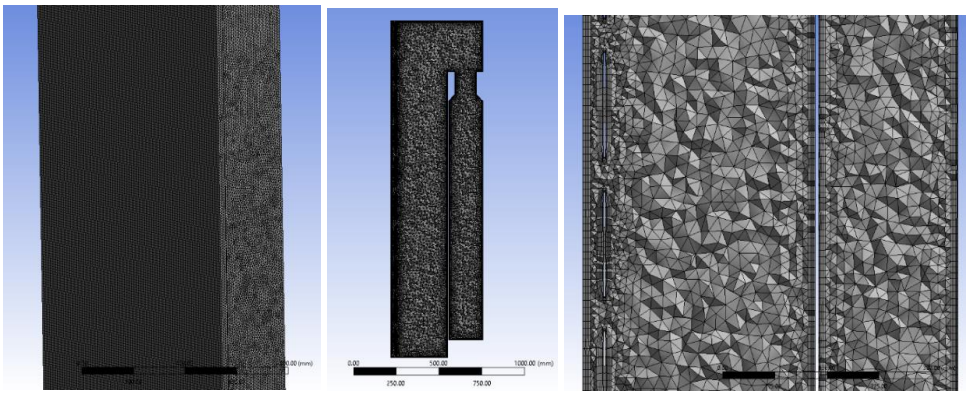

Figure 5. 2.95 million tetrahedral elements of the GTC a) front view b) longitudinal section c) closeup longitudinal section

The airflow modelling was based on the RNG k- ε turbulence model with Enhanced Wall Functions for near-wall airflow treatment [14]. This approach can predict with accuracy both the free stream airflow and the airflow through the orifices. The radiation model used was the Surface to Surface (S2S) model, and the solar load taken in consideration was 800 W/m^2 for direct solar irradiation and 150 W/m^2 for diffuse solar irradiation, the calculation being achieved for Bucharest (Romania).

Analyzing the air flows for the six simulations shown below in Table 4, it can be seen that due to the distance of 50 mm between the absorber plate and the glass, air flow rates of around 150m^3/h lead to a reduced heat collection from the absorber plate.

Table 4: Temperature and velocity CFD simulation for GTC

50 mm	158m3/h	203m3/h	250m3/h	296m3/h	354m3/h	397m3/h
Temperature	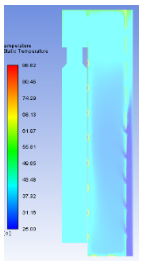	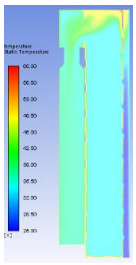	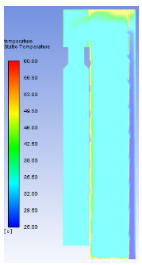	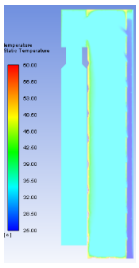	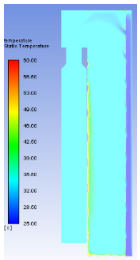	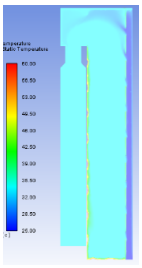

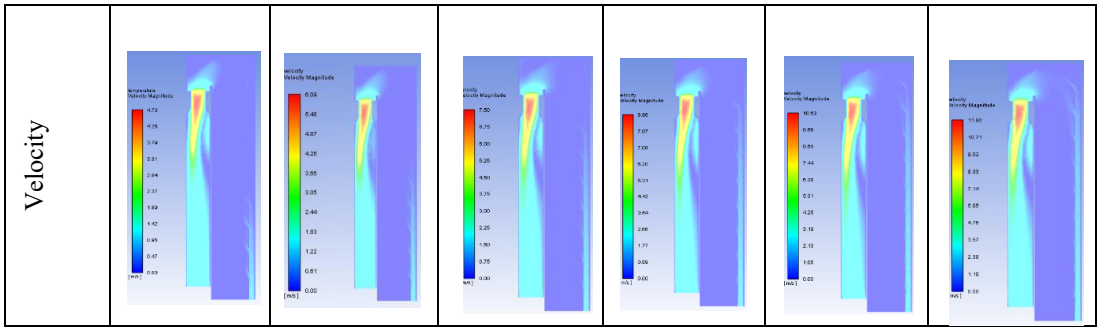

The experimental – numerical comparisons in terms of solar collector heat flux (Figure 6) show that the simulations overestimate the heat transfer inside the GTC. This is to be expected because higher values of solar radiation have been introduced in the numerical model than experimental values recorded during the measurements. On the other hand, there is more or less the same trend of variation with air flow rate for both experimental and numerical data.

Regarding the comparisons of solar collector global efficiency (Figure 7), the values are much closer but it is clear that there is a need for an improvement of the numerical model, at least in terms of boundary conditions for the intensity of solar radiation.

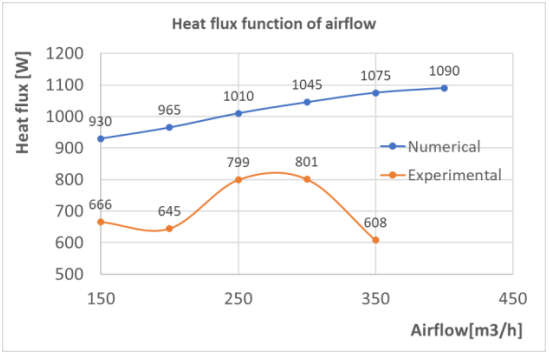

Figure 6 Numerical and experimental heat flux

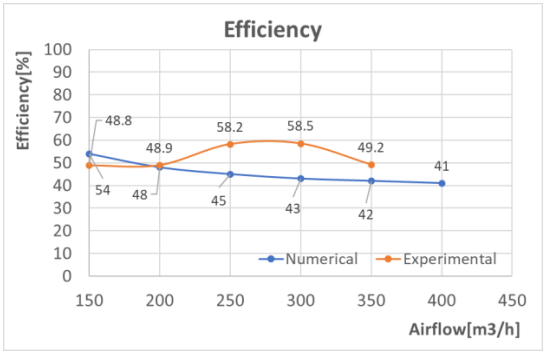

Figure 7 Numerical and experimental efficiency

6. Discussion on numerical results

Analysing the GTC proposed in the CAMBI research center, it can be observed that its global efficiency numerically assessed is maintaining around an average value of 45%.

In the case of the numerical study, it is observed that the heat transfer increases constantly with the air flow rate, appearing however a visible reduction of this increase for air flow rates of approximately 350-400 m^3/h.

Finally, the differences between the numerical and experimental values result also from different operating conditions (solar radiation and wind speed), conditions that will have to be harmonized.

7. Conclusion

The results obtained in the numerical study for the GTC prototype proposed within the CAMBI research center, correlated with the experimental studies, show us the potential of these types of GTC to be integrated in buildings in order to preheat fresh air in ventilation systems, leading to important energy savings.

In addition, the results show in both cases that for this GTC with a distance of 50 mm between the absorber plate and the glass the air flow rate of around 300 m^3/h represents the limit value for reaching the best values in terms of global efficiency.

These results will also help us to implement new strategies in the following projects and researches dealing with “smart facades” and integration of phase change materials in solar collectors.

8. Acknowledgement
This study was financed by Romanian National Authority for Scientific Research, project CIA-CLIM "Smart buildings adaptable to the climate change effects" PN-III-P1-1.2-PCCDI-2017-0391.

9. References

[1] Global Energy Review 2020. OECD, 2020.

[2] R. G. Newell and D. Raimi, "Global Energy Outlook Comparison Methods: 2019 Update," Resour. Futur., 2019.

[3] G. S. R. UN Environmental and International Energy Agency, "Towards a zero-emission, efficient, and resilient buildings and construction sector," 2017.

[4] K. Hami, B. Draoui, and O. Hami, "The thermal performances of a solar wall," *Energy*, vol. **39**, no. 1, pp. 11–16, Mar. 2012,

[5] C.-M. Lai and S. Hokoi, "Solar façades: A review," *Build. Environ.*, vol. **91**, pp. 152–165, Sep. 2015,

[6] D. N. Nkwetta and F. Haghighat, "Thermal energy storage with phase change material—A state-of-the art review," *Sustain. Cities Soc.*, vol. **10,** pp. 87–100, Feb. 2014, DOI:10.1016/j.scs.2013.05.007.

[7] A.-S. Bejan, A. Labihi, C.-V. Croitoru, F. Bode, and M. Sandu, "Experimental Investigation of the Performance of a Transpired Solar Collector Acting as a Solar Wall," in Proceedings of *SWC2017/SHC2017*, 2017, pp. 1–10,

[8] A.-S. Bejan, C. V. Croitoru, and F. Bode, "Preliminary numerical studies conducted for the numerical model of a real transpired solar collector with integrated phase changing materials," *E3S Web Conf.*, vol. **111**, p. 03047, Aug. 2019,

[9] A.-S. Bejan, F. Bode, C. Teodosiu, C. V. Croitoru, and I. Năstase, "Numerical model of a solar ventilated facade element: experimental validation, final parameters and results," *E3S Web Conf.*, vol. **85**, p. 02013, Feb. 2019,

[10] C. Croitoru, "INNOVATIVE SOLAR WALL PERFORMANCE STUDY FOR LOW ENERGY BUILDINGS APPLICATIONS," in *International Multidisciplinary Scientific GeoConference Surveying Geology and Mining Ecology Management, SGEM*, Jun. 2014, vol. **1**, no. 4, pp. 307–314,

[11] C. Croitoru, "HEAT TRANSFER ANALYSIS FOR A TRANSPIRED SOLAR COLLECTOR NUMERICAL MODEL," Jun. 2011,

[12] L. Gao, H. Bai, and S. Mao, "Potential application of glazed transpired collectors to space heating in cold climates," *Energy Convers. Manag.*, vol. **77**, pp. 690–699, Jan. 2014,

[13] X. Wang, B. Lei, H. Bi, and T. Yu, "A simplified method for evaluating thermal performance of unglazed transpired solar collectors under steady state," *Appl. Therm. Eng.*, vol. **117**, pp. 185–192, May 2017,

[14] F. Bode, A. Meslem, C. Patrascu, and I. Nastase, "Flow and wall shear rate analysis for a cruciform jet impacting on a plate at short distance," *Prog. Comput. Fluid Dyn. An Int. J.*, vol. **20**, no. 3, p. 169, 2020,